Phys. JETP **21**, 302 (1965)].

[3]S. M. Hamberger and M. Friedman, Phys. Rev. Lett. **21**, 674 (1968); S. M. Hamberger and J. Jancarik, Phys. Fluids **15**, 825 (1972).

[4]D. Dimok and E. Mazucato, Phys. Rev. Lett. **20**, 713 (1968).

[5]A. Hirose, I. Alexeff, W. D. Jones, S. T. Kush, and K. E. Lonngren, Phys. Rev. Lett. **25**, 1563 (1970).

[6]N. I. Elagin and S. D. Fanchenko, Zh. Eksp. Teor. Fiz. **67**, 1355 (1974) [Sov. Phys. JETP **40**, 674 (1975)].

[7]E. A. Jackson, Phys. Fluids **3**, 786 (1960).

[8]Duk-In Choi and W. Horton, Jr., Phys. Fluids **17**, 2048 (1974).

[9]W. Horton, Jr., Duk-In Choi, and R. A. Kock, Phys. Rev. A **14**, 424 (1976).

[10]Y. Kawai and Ch. Hollenstein, Phys. Lett. **59A**, 353 (1976).

[11]H. Tanaca, A. Hirose, and M. Koganei, Phys. Rev. **161**, 94 (1967).

[12]N. Th. Karatzas, A. J. Anastassiadio, and K. Papadopoulos, Phys. Rev. Lett. **35**, 33 (1975).

[13]B. B. Kadomtsev, *Plasma Turbulence* (Academic, New York, 1965).

[14]When L was shorter than 5 cm, a discrete spectrum, which consists of a number of higher harmonics, was observed, as reported in Ref. 11. In this case, the fundamental mode frequency, f_1, agreed with C_s/L and, in addition, was proportional to $(1/L)$. Therefore, although the spectrum becomes continuous for large L, qualitatively the linear dispersion relation can be considered to be useful.

[15]Parameters in the theory are those during the turbulence. The electron distribution was measured by the energy analyzer placed just behind the grid. However, no remarkable change was observed in the presence of the turbulence. On the other hand, the measurement of T_i was made in the absence of the turbulence. However, T_i during the turbulence would be replaced by that in the absence of the turbulence since we did not have any magnetic fields to confine the ions.

[16]R. D. Bengtson, K. W. Gentle, J. Jancarik, S. S. Medley, P. Nielson, and P. Phillips, Phys. Fluids **18**, 710 (1975).

[17]R. Z. Sagdeev and A. A. Galeev, in *Nonlinear Plasma Theory*, edited by T. M. O'Neil and D. L. Book (Benjamin, New York, 1969), p. 103.

Measurement of Density Modification of Laser-Fusion Plasmas

H. Azechi, S. Oda, K. Tanaka, T. Norimatsu, T. Sasaki, T. Yamanaka, and C. Yamanaka

Institute of Laser Engineering, Osaka University, Suita, Osaka 565, Japan

(Received 25 August 1977)

Density profile of the glass-microballoon plasma irradiated by Nd laser with intensity of 10^{16} W/cm^2 was measured by newly developed microscopic interferography. The existence of strong density modification by intense radiation pressure was clearly indicated.

The hydrodynamic behavior of laser-produced plasmas is essentially important for laser fusion research, because absorption mechanisms of laser light depend on the density profile of the plasma. Recent theoretical and computational investigations[1-5] show that the density gradient near the critical density ($n_c = 10^{21}$ cm^{-3} for Nd laser) is dramatically steepened by intense radiation pressure.[6] Because of the density steepening, the resonant absorption[7,8] becomes an effective absorption mechanism while the efficiency of the parametric instability and the classical absorption are reduced. There have been a number of experimental studies[9-13] on the density profile of laser-produced plasmas. Density cavities produced by the radiation pressure were observed in in recent experiments using CO_2 laser ($\lambda = 10.6$ μm).[12,13] We have reported the existence of the density modification by Nd laser ($\lambda = 1.06$ μm) with an indirect method, that is, spectrum measurement of backscattered light.[14]

In this Letter, we present the observation of the density profile of the plasma irradiated by Nd laser with an intensity of 10^{16} W/cm^2 and infer the existence of the strong density modification.

The glass laser "Gekko II," two-beam system[15] was used to irradiate a glass-microballoon target, the diameter of which was 50–58 μm. The oscillator was a yttrium aluminum garnet laser, mode locked by a saturable dye, which was followed by nine rod-type amplifiers. The diameter of the final rod was 80 mm. The output energy was typically 15 J per beam and the pulse duration was 30 psec full width at half-maximum. The prepulse energy was minimized by two saturable dye cells in the early stage of the amplifiers. The energy of the prepulse was less than 20 μJ. The amplified spontaneous emission was below 1 mJ. The soft aperture and the vacuum spatial filters were used to get a clean beam. The f number of the focusing lens was 1.2. The typical focusable power was 10 J in 50 μm diam.
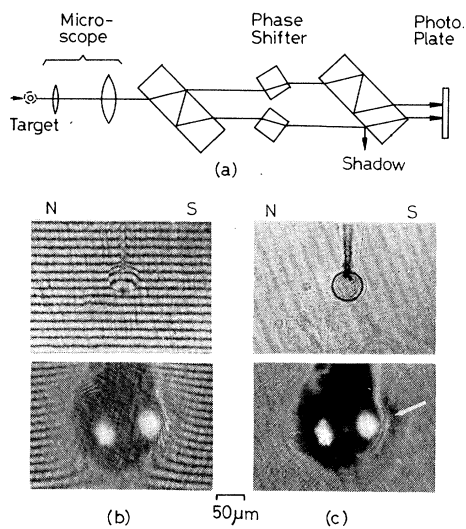
FIG. 1. (a) Schematic diagram of microscopic inter-ferometer. The arrow shows the optical path of the probing light. Spatial resolution is better than 2 μm. (b) Interferograph and (c) simultaneously obtained shadowgraph. Top figures were taken before the laser irradiation and the bottom figures were taken at 370 psec after. Two beams are focused from north and south sides. Intensities of the north and south beams are 10^{15} and 10^{16} W/cm^2, respectively. Bright spots are due to the second-harminic radiation from the plasma.

The laser intensity was over 10^{16} W/cm^2 on the target.

The density profile of the ablating plasma was observed by interferography and shadowgraphy. In order to provide a probing light, a small portion of the main laser light was split off and frequency doubled by a potassium dihydrogen phosphate (KDP) crystal. The pulse duration of the light entering into the KDP was compressed by a dye-amplifier chain. Figure 1(a) shows the schematic diagram of the interferometer which was newly developed. The probing light, after passing through the target, is divided into two beams. The phase fronts of each beam were spatially shifted by phase shifters. The one beam which passes the target interferes with the other which passes through vacuum near the target. The image of the target is magnified 50 times on Polaroid No. 105 film by a microscope. Thie system has very high spatial resolution and is easy to construct. In addition, a shadowgraph can be obtained simultaneously.[10,11] The spatial and temporal resolutions were better than 2 μm and 20 psec, respectively. We defined the time origin as the time when the fringe shift and the shadow of the plasma first appeared. Therefore the

time origin indicates the onset time of the laser irradiation. The electron temperature was measured by Ross filter method. The measurable spectral range was from 1 to 80 keV. Time of flight of ions was measured by charge collectors. The cold- and hot-electron temperatures were typically 1 and 15 keV, respectively, at the laser intensity of 10^{16} W/cm^2.

We have measured the time history of the density profile of the ablating plasma. Figure 1(b) shows the typical interferographic result at 370 psec after the onset of the laser irradiation. These photographs were taken under the condition of two-beam irradiation, where the light intensity of the south beam was 10^{16} W/cm^2 and that of the north beam was 10^{15} W/cm^2. The time difference between two beams was less than 30 ps. The bright spots which are at 7 μm from the initial wall of the microballoon are due to the second-harmonic radiation from the plasma and correspond to the laser-energy deposition region.[16] In the south side of the Fig. 1(b), the fringe shift strongly changed near the bright spot. The shadowgraph simultaneously observed is shown in Fig. 1(c). A dark arc (indicated by an arrow) corresponds to the region where the fringe shift becomes steep. Since the light intensity of the shadowgraph is proportional to the second derivative of the electron density with respect to space,[17] the dark arc indicates that the density gradient changes at this region. The integrated density profile in the south side $\int n_e dl$, where dl is the plasma depth, were converted to the radial density profile by Abel inversion as shown in Fig. 2. A density shelf propagating radially into the low-density region appeared at ~10^{20} cm^{-3}. This shelf was observed up to 400 psec. Along the laser axis, the density gradient at the higher-density region was steeper than that of the lower-density region. The temporal change of the axial density profile is shown in Fig. 3(a). These density profiles are separated into the short- and the long-density-scale-length regions. The density scale length was defined as the distance where the density decreases by a factor of e^{-1}. The temporal change of the short and the long scale lengths, L_1 and L_2, are shown in Fig. 3(b). The time derivative of the short scale length, dL_1/dt, was about 2.5×10^6 cm/s, and dL_2/dt was more than 10^7 cm/s. The short scale length under the laser irradiation was extrapolated to be $l \sim 2$ μm. During the period of the laser irradiation, the short-scale-length region was not able to be detected, because the refraction of the probing light was
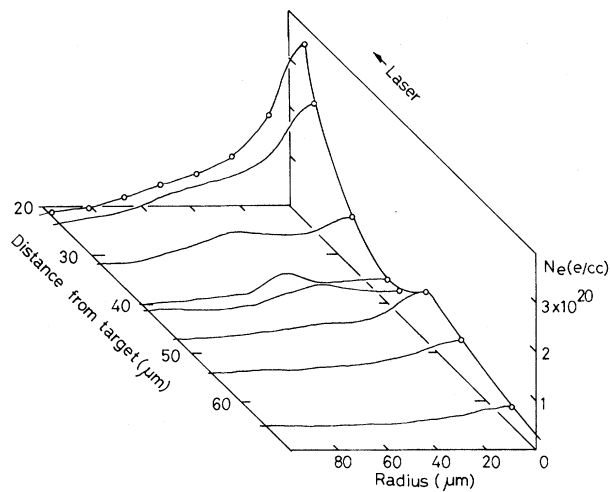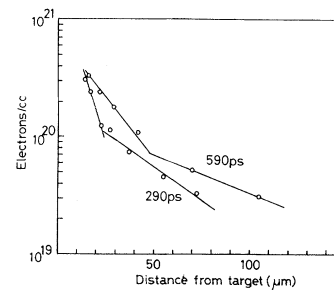
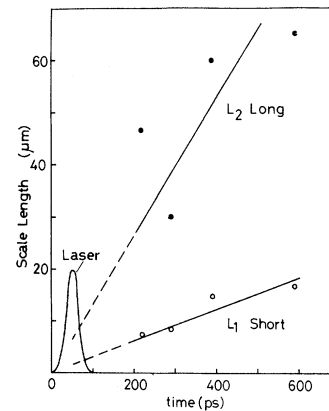FIG. 2. Radial density profile at 370 psec after the laser irradiation.

FIG. 3. (a) Temporal change of axial density profile. The density gradient at the higher-density region is steeper than that of the lower-density region. (b) Density scale length vs time. L_1 and L_2 show short and long scale lengths, respectively. The critical density surface is in the short–scale-length region.

enhanced by the large density gradient, so that the light passing through the short–scale-length region could not enter the microscope objective. More than 600–700 psec after the laser irradiation, the long–scale-length region became unobservable because of the radial expansion.

The isothermal rarefaction solution shows that the density scale length is 9 μm at 30 psec (pulse width), for a temperature of ~ 1 keV and ionization number of ~ 10. The extrapolated scale length is shorter than that value and the observed density profiles differ from the rarefaction profile.

The axial density profile can be explained by the density modification due to the radiation pressure. The theory of the density modification which takes account of the plasma flow has recently been given by Lee et al.[4] They showed that two shelves, upper and lower density, are formed at both sides of the critical density surface. The transition region from the upper to the lower shelf has a very steep density gradient. In the frame moving with the discontinuity, the flow is accelerated from subsonic to supersonic at the discontinuity. The jumps of the density and the flow velocity increase with increasing of the radiation pressure. The density gradient at the discontinuity is too large to detect at an early period of time, but at the later time this discontinuity breaks down so as to be observable. We presume that the short– and the long–scale-length regions correspond to the discontinuity surface and the rarefaction tail, respectively. In the present experiments, the ratio of the quivering electron

velocity v_0 to the electron thermal velocity v_e is ~ 2. At this ratio, the predicted upper-shelf density $n = 3n_c$ is too high to detect with the present measuring system. But the lower-shelf density is predicted to be $(0.13-0.04)n_c$, which is in good agreement with the experimental value ($\sim 0.1n_c$).

In conclusion, the existence of density modification due to the radiation pressure was clearly indicated. The density profile of the ablating plasma consisted of the short– and the long–density-scale regions joined by the density shelf. The density scale length near the critical density was very short in comparison with the unperturbed profile. These results show that the radiation pressure is a dominant factor in a determination of the density profile and the resonant absorption will become an important absorption mechanism in the laser fusion experiment.

The authors are grateful to Dr. K. Nishihara for discussions. They also wish to thank H. Hashizume, K. Hashizume, H. Kitamura, A. Tsujimoto,

and T. Kanabe for their technical assistance.

[1]R. E. Kidder, in *Proceedings of Japan–U.S. Seminar on Laser Interaction with Matter*, edited by C. Yamanaka (Tokyo International Book Co., Tokyo, 1975), p. 331.

[2]F. W. Forslund, J. M. Kindel, K. Lee, E. L. Lindman, and R. L. Morse, Phys. Rev. A **11**, 679 (1975).

[3]K. G. Estabrook, E. J. Valeo, and W. L. Kruer, Phys. Fluids **18**, 1151 (1975).

[4]K. Lee, D. W. Forslund, J. M. Kindel, and E. L. Lindman, Phys. Fluids **20**, 51 (1977).

[5]P. Mulser and C. van Kessel, Phys. Rev. Lett. **38**, 902 (1977).

[6]H. Hora, Phys. Fluids **12**, 182 (1969).

[7]V. L. Ginzburg, *Propagation of Electromagnetic Waves in Plasmas* (Pergamon, New York, 1970), p. 260.

[8]R. B. White and F. F. Chen, Plasma Phys. **16**, 565 (1974).

[9]D. T. Attwood, L. W. Coleman, and D. W. Sweeney, Appl. Phys. Lett. **26**, 616 (1975).

[10]H. Azechi, Y. Sakagami, T. Yamanaka, and C. Yamanaka, Appl. Phys. Lett. **30**, 187 (1977).

[11]H. Azechi, Y. Sakagami, T. Yamanaka, and C. Yamanaka, J. Phys. Soc. Jpn. **42**, 1362 (1977).

[12]T. P. Donalson and I. P. Spalding, Phys. Rev. Lett. **36**, 467 (1976).

[13]J. L. Bocher, J. P. Elie, J. Martineau, M. Rabeau, and C. Patou, in Proceedings of the Fourth Workshop on Laser Interaction and Related Plasma Phenomena, Rensselaer Polytechnic Institute, Troy, New York, November, 1976 (unpublished).

[14]C. Yamanaka, T. Yamanaka, J. Mizui, and N. Yamaguchi, Phys. Rev. A **11**, 2138 (1975).

[15]C. Yamanaka *et al.*, Institute of Laser Engineering, Osaka University, Annual Progress Report No. ILE-APR-76, 1976 (unpublished).

[16]S. Jackel, J. Albritton, and E. Goldman, Phys. Rev. Lett. **35**, 514 (1975).

[17]U. Ascoli Bartoli, in *Proceedings of the Second Conference on Plasma Physics and Controlled Nuclear Fusion Research, Culham, England, 1965* (International Atomic Energy Agency, Vienna, Austria, 1966), p. 287.

Soliton Generation at Resonance and Density Modification in Laser-Irradiated Plasmas

Hsing-Hen Chen and Chuan-Sheng Liu

Department of Physics and Astronomy, University of Maryland, College Park, Maryland 20742

(Received 29 June 1977)

Analytic results are obtained for generation of solitons and their effects on density-profile modifications at critical density for resonance absorption process.

For a laser beam of frequency ω_0 obliquely incident onto a nonuniform plasma slab with polarization in the plane of incidence, there is a component of the electric field along the density gradient driving the density oscillation. Because of Budden tunneling, the residual electric field beyond the cutoff can drive the plasma wave at resonance where $\omega_p(x) = \omega_0$. This transformation of the electromagnetic wave into electrostatic waves which are subsequently absorbed by the plasma particles constitutes an important absorption mechanism of the laser radiation.[1]

In the usual linear theory, a fixed density profile is assumed and the modification of the density profile by the large-amplitude plasma wave generated at resonance is neglected.[2] In reality, even for a relatively weak pump wave, the resonantly driven plasma wave can significantly modify the density profile near the critical density region by the ponderomotive force.[3-6] Because of the localized structure of the field near the resonance, the ponderomotive pressure tends to drive the plasma out of the resonance region, thus depleting the local plasma density, forming a caviton (soliton). The successive generation of solitons and their subsequent downward motion along the density gradient results in a quasistationary density step with steep density gradient.[3,4,6] The formation of this sharp density step can stabilize many parametric processes,[3,4] affecting the absorption and scattering of laser light

In this Letter, we present an analytic theory of these nonlinear processes of soliton generations and profile modifications at the resonance. Threshold conditions for N-soliton formation are obtained. A closely related problem is the saturation of the linearly transformed wave. In the linear theory, the thermal convection of the plasma wave and its subsequent Landau damping provides the saturation after a time $t_c \approx (L/\lambda_D)^{2/3}\omega_{pe}^{-1}$, where L is the initial (unmodified) density scale length and $\lambda_D = (T/4\pi n e^2)^{1/2}$ is the Debye length. Because the soliton generation involves ion motion which takes place after several ion plasma
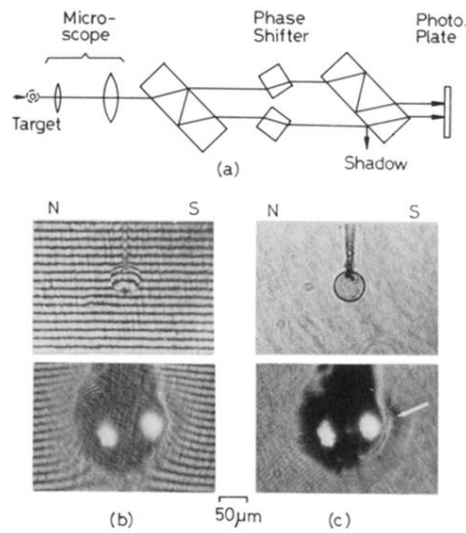
Micro-
scope

Phase
Shifter

Photo.
Plate

Target

Shadow

(a)

N   S   N   S

50μm

(b)   (c)

FIG. 1. (a) Schematic diagram of microscopic inter-
ferometer. The arrow shows the optical path of the
probing light. Spatial resolution is better than 2 μm.
(b) Interferograph and (c) simultaneously obtained
shadowgraph. Top figures were taken before the laser
irradiation and the bottom figures were taken at 370
psec after. Two beams are focused from north and
south sides. Intensities of the north and south beams
are 10^{15} and 10^{16} W/cm^2, respectively. Bright spots are
due to the second-harminic radiation from the plasma.